An Isolable Azide Adduct of Titanium(II) Follows Bifurcated Deazotation Pathways to an Imide

Anders Reinholdt,^{a,‡} Seongyeon Kwon,^{b,c,‡} Mehrafshan G. Jafari,^a Michael R. Gau,^a Patrick J. Caroll,^a Chad Lawrence,^a Jun Gu,^a Mu-Hyun Baik,^{c,b,*} Daniel J. Mindiola^{a,*}

- ^a Department of Chemistry, University of Pennsylvania, 231 South 34th Street, Philadelphia, PA 19104 (USA), E-mail: mindiola@sas.upenn.edu.
- ^b Department of Chemistry, Korea Advanced Institute of Science and Technology (KAIST), Daejeon 34141 (Republic of Korea), E-mail: mbaik2805@kaist.ac.kr.
- ^c Center for Catalytic Hydrocarbon Functionalizations, Institute for Basic Science (IBS), Daejeon 34141 (Republic of Korea), E-mail: mbaik2805@kaist.ac.kr.

ABSTRACT: AdN₃ (Ad = 1-adamantyl) reacts with the tetrahedral Ti^{II} complex [(Tp^{'Bu,Me})TiCl] (Tp^{'Bu,Me} = hydrotris(3-*tert*-butyl-5-methylpyrazol-1-yl)borate), to generate a mixture of an imide complex, [(Tp^{'Bu,Me})TiCl(NAd)] (**4**), and an unusual and kinetically stable azide adduct of the group 4 metal, namely [(Tp^{'Bu,Me})TiCl(γ-N₃Ad)] (**3**). In these conversions, the product distribution is determined by the relative concentration of reactants. In contrast, the azide adduct **3** forms selectively when a masked Ti^{II} complex (N₂ or AdNC adduct) reacts with AdN₃. Upon heating, **3** extrudes dinitrogen in a unimolecular process proceeding through a titanatriazete intermediate to form the imide complex **4**, but the observed thermal stability of the azide adduct ($t_{1/2}$ = 61 days at 25 °C) is at odds with the large fraction of imide complex formed directly in reactions between AdN₃ and [(Tp^{'Bu,Me})TiCl] at room temperature (ca. 50% imide with a 1:1 stoichiometry). A combination of theoretical and experimental studies identified an additional deazotation pathway, proceeding through a bimetallic complex bridged by a single azide ligand. The electronic origin of this deazotation mechanism lies in the ability of azide adduct **3** to serve as a π-backbonding metallaligand toward free [(Tp^{'Bu,Me})TiCl]. These findings unveil a new class of azide-to-imide conversions for transition metals, highlighting that the mechanisms underlying this common synthetic methodology may be more complex than conventionally assumed, given the concentration dependence in the conversion of an azide into an imide complex. Lastly, we show how significantly different AdN₃ reacts when treated with [(Tp^{'Bu,Me})VCl].

INTRODUCTION

The formation of a transition metal imide complex via extrusion of dinitrogen from an organic azide is a classic reaction that continues to garner interest in the coordination chemistry community, 1-14 but also underpins organic transformations such as nitrene homocoupling to azoarenes, 15,16 isocyanide-nitrene coupling to carbodiimides,17,18 alkenenitrene coupling to aziridines, 19-21 [2+2+1] alkyne-nitrene coupling to pyrroles, 22-24 and C-H bond amination. 25-32 The oxo-wall, introduced by Gray and Ballhausen,33-35 delimits the electronic structure of stable oxo and imide complexes: In tetragonal geometries, valence electron counts beyond d^2 lead to the occupation of M-N π^* orbitals, which destabilizes the M≡N triple bonds, whereas valence electron counts up to d^4 are stable in low-coordinate geometries. A reverse situation exists for organoazide adducts, which gain stability when valence electron counts exceed d^4/d^6 ; these complexes prevail among late transition metals. 15,16,30,36-51 The conversion of an organoazide into an imide complex, although a seemingly simple metal-promoted deazotation reaction, has only been studied mechanistically by few groups. In 1995, Bergman^{52,53} and Cummins⁵⁴ isolated y-organoazide adducts of the early transition metal fragments Ta^{III} and VIII (we label organoazides starting from the organic

substituent: $RN_{\alpha}N_{\beta}N_{\gamma}$). These complexes are kinetically stable, even though d^2 fragments, naively, should be devoid of electronic impediments for deazotation. More recently, Chang and Arnold have expanded upon these studies using VIII and NbIII, respectively (Chart 1, A). Interestingly, group 5 transition metals continue to define the border for isolable organoazide adducts of mononuclear d2 fragments. 18,55,56 Given the decreasing d-orbital energies within transition series, this poses the question of whether divalent group 4 metals are too reducing to stabilize organoazides as ligands. As for the conversion of organoazides into imide complexes, a mechanism involving the formation and capture of free nitrene has sporadically been suggested. 16,55,57 But in general, mononuclear imide complexes (M≡NR) are assumed to form via simple mono- or binuclear pathways through intermediates where the metal:azide ratio is unity (examples: Chart 1, B). 52-54,58-61 Deviation from this ratio has been suggested for multimetallic systems such as Bergman's $[Cp_2M(\mu-N^tBu)(\gamma,\gamma;\mu-N_3Ph)IrCp^*]$ complexes (M = Zr,Hf),62,63 but in this case, it is the binuclear nature of the complexes that dictates a 2:1 metal:azide ratio. Herein, we report how a tetrahedral, high-spin Ti^{II} complex binds an organic azide to afford mixtures of the corresponding azide and imide products (Chart 1, C), the ratio of which is determined by the relative concentrations of the reactants. The azide adduct extrudes N₂ sluggishly even at elevated temperatures ($t_{1/2}$ = 43 h at 50 °C) in a unimolecular deazotation pathway most likely proceeding through a titanatriazete intermediate, as originally proposed by Bergman. However, an unusual complementary mechanism, operating through two metal centers and π -backbonding to the bridging azide ligand, expedites deazotation at lower temperatures, as verified by kinetic and quantum chemical studies. Our study not only demonstrates how important the effect of concentration of the metal complex is on the pathway for deazotation but also shows that the order of addition of reagents (metal complex to azide *versus* the reverse) should be considered when optimizing reaction conditions.

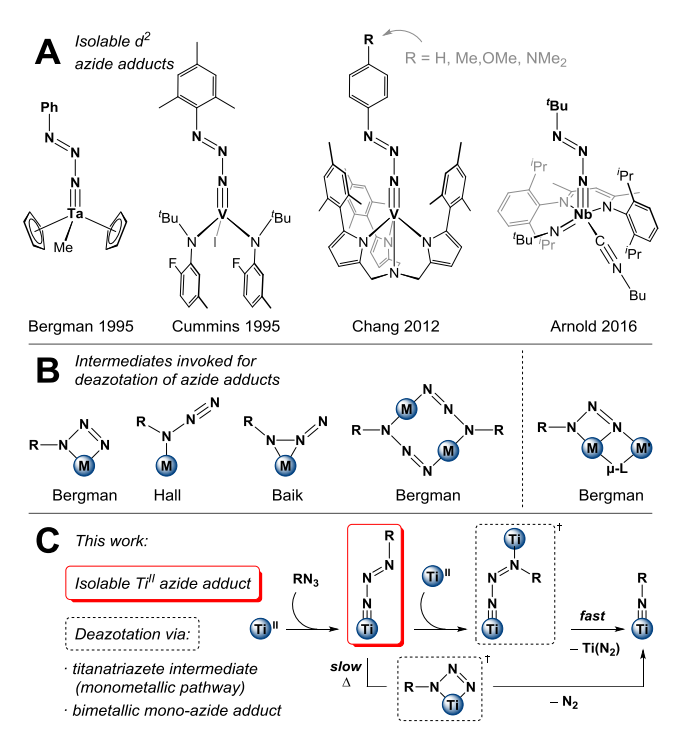


Chart 1. A: Isolable azide adducts of d^2 metal fragments, **B:** Intermediates proposed in deazotation of azide adducts. **C:** This work showing an isolable organoazide adduct of Ti^{II} undergoing deazotation to form a terminal imide complex via 1) a bimetallic mono-azide intermediate, or 2) a monometallic titanatriazete intermediate.

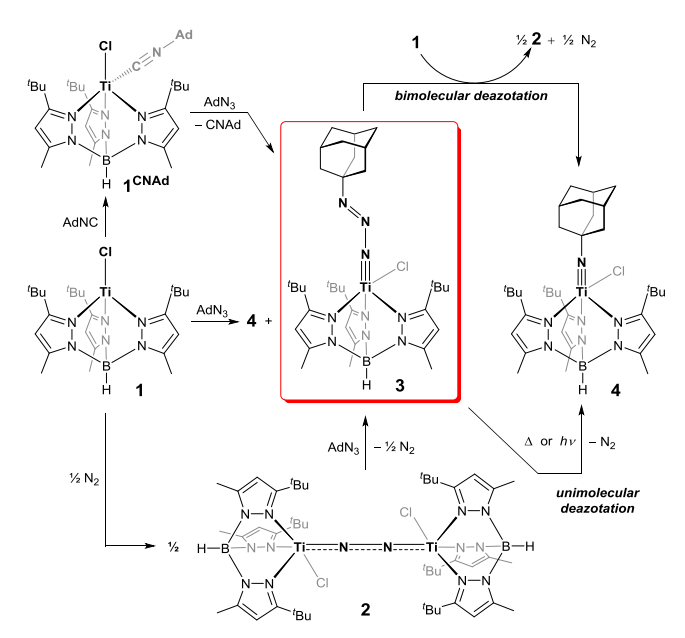
RESULTS AND DISCUSSION

Isolation of an Azide Adduct of Ti^{II} (3)

Classic synthetic strategies toward Ti^{II} complexes rely on the maximization of the coordination number and/or installation of π -acidic ligands in order to stabilize the large and reducing Ti^{II} ion. In the pursuit of alternative ligand designs, we recently prepared a tetrahedral and high-spin Ti^{II} complex bearing redox-innocent ligands, namely [(Tp^(Bu,Me))TiCl] (1, Tp^(Bu,Me) = hydrotris(3-tert-butyl-5-methylpyrazol-1-yl)borate).⁶⁴ This sterically accessible and highly reducing d^2 complex forms adducts with π -acids such as AdNC and N₂, [(Tp^(Bu,Me))TiCl(CNAd)] (1^{CNAd}) and [{(Tp^(Bu,Me))TiCl}₂(μ -N₂)] (2), respectively, whereas it quantitatively extrudes N₂ upon reaction with Me₃SiN₃ to afford the prototypical Ti^{IV} silylimide complex, [(Tp^(Bu,Me))TiCl(NSiMe₃)].⁶⁴ Although this

entry to titanium imide complexes is universal,65-72 the unique geometry of 1 prompted us to further explore its reactivity toward other azides: Under an Ar atmosphere, treatment of a benzene solution of 1 with the organic azide, AdN₃, led to a dark yellow two-component reaction mixture (Scheme 1). ¹H NMR spectroscopy revealed two diamagnetic species; the first, $[(Tp^{tBu,Me})TiCl(\gamma-N_3Ad)]$ (3), displayed a single set of pyrazole resonances, in line with rapid interconversion on the ¹H NMR timescale. In contrast, the second species, [(Tp^{tBu,Me})TiCl(NAd)] (4), displayed two sets of pyrazole resonances in line with C_s symmetry in solution. When prepared using a 1:1 ratio between AdN₃ and **1**, the products form in similar amounts, although the exact product distribution also depends on the order of addition of reactants (vide infra). Upon heating 3 to 80 °C over several hours, reaction mixtures progressed cleanly to the bright orange C_s symmetric product 4; the same outcome resulted upon irradiation with the full spectrum of a Xe lamp over tens of minutes in solution or solid state phases.

Searching for an alternative, but selective, entry to the metastable species 3, we examined $\pi\text{-acid}$ adducts of 1 as sources of a masked $^{72\text{-}76}$ Ti II fragment. Thus, when $\mathbf{1}^{\text{CNAd}}$ or 2 reacts with AdN3 in benzene (under either N2 or Ar), metastable 3 forms in near quantitative spectroscopic yield with concomitant release of AdNC or N2, respectively. Notably, the isocyanide ligand in $\mathbf{1}^{\text{CNAd}}$ does not enact nitrene coupling to generate a carbodiimide, AdNCNAd, $^{17,18,77\text{-}80}$ contrasting with the facile P-atom transfer reactivity between $\mathbf{1}^{\text{CNAd}}$ and Na(OCP), which affords the cyanophosphide complex, [(Tp^{tBu,Me})Ti($\eta^3\text{-PCNAd})$]. 81



Scheme 1. AdN₃ reacts with Ti^{II} complex **1** to generate azide adduct **3** and imide complex **4**, whereas treatment of AdN₃ with the isocyanide complex $\mathbf{1}^{\text{CNAd}}$ or dinitrogen complex **2** selectively affords **3**. Deazotation of **3** to **4** occurs upon heating, photolysis, or *via* treatment with an extra equivalent of **1**. To avoid formation of **2**, all reactions involving **1** were carried out under Ar; the remaining reactions proceed equally well under N₂/Ar.

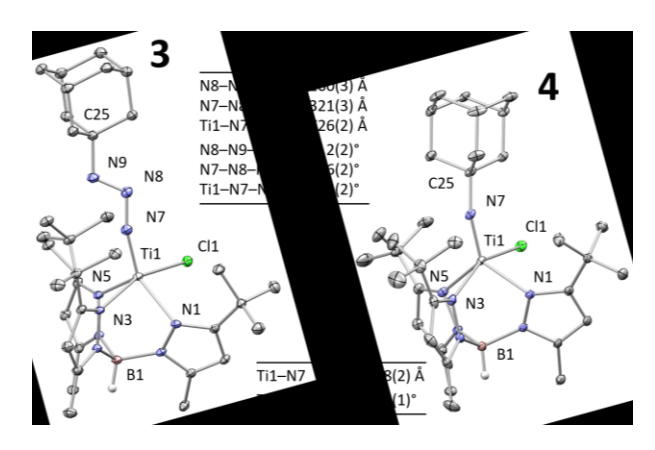


Figure 1. Thermal ellipsoid plots of **3** and **4** (50% probability). Co-crystallized pentane (**3**, **4**) and disorder in one Ad group for complex **4** are omitted.

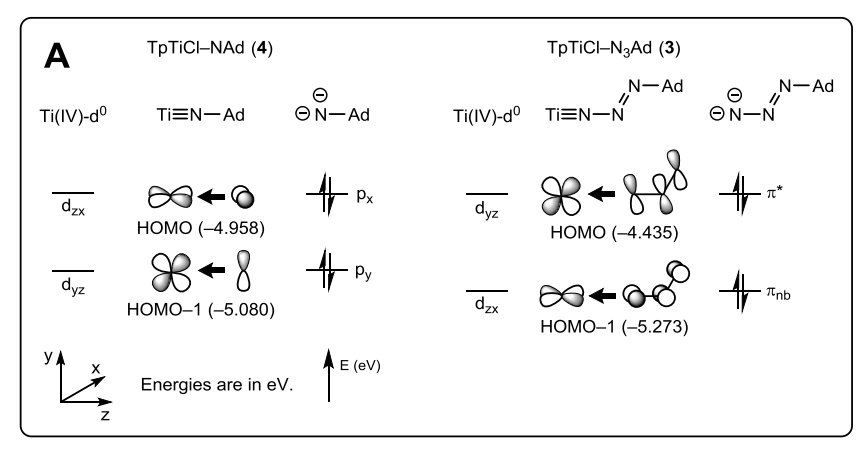
Both products, 3 and 4, could be isolated from the reaction mixtures upon removal of the solvent and recrystallization from pentane. This affords dark yellow crystals of 3 (70% isolated yield) or bright orange crystals of 4 (70% isolated yield), depending on the synthetic route taken. X-ray crystallographic characterization revealed the thermodynamic product to be the anticipated mononuclear titanium imide complex, [(Tp^{tBu,Me})TiCl(NAd)] (4, see **Figure 1**). This five-coordinate complex has a geometry index, $\tau_5 = 0.50,^{82}$ midway between idealized square pyramidal and trigonal bipyramidal geometries, and the short Ti1-N7 distance is in line with a {Ti≡N} multiple bond. The angle around N7 (160.1(1)°) deviates notably from linearity, presumably due to steric repulsion between the Ad and 'Bu groups (shortest H···H separation: 2.22 Å), which in turn impedes rotation about the Ti \equiv N spine and enforces the C_s symmetry observed on the ¹H/¹³C NMR timescales. More surprisingly, crystallographic characterization of the metastable product revealed an adduct between the Ti^{II} complex and intact AdN₃, namely $[(Tp^{tBu,Me})TiCl(\gamma-N_3Ad)]$ (3). It is notable that while mononuclear late transition metal organoazide adducts display a wealth of coordination modes (α-N₃R,^{30,36}- $^{38,44-48}$ γ - $N_3R_1^{15,16,37}$ $\beta_1\gamma$ - N_3R^{49-51}), early transition metals invariably form γ-N₃R adducts in which N₂ extrusion requires extensive structural reorganization. The geometry index of 3 indicates a distorted five-coordinate structure ($\tau_5 = 0.39$) that approaches a square pyramidal configuration more than imide complex 4. The Ti1-N7 distance in 3 is 1.6% longer than the $\{Ti\equiv N\}$ triple bond in 4, while the angle around N7 (165.4(2)°) is closer to linearity. Bond distances in the {N₃} moiety fall in the range between N-N double and

single bonds (informative metrics: HN=NH: 1.230 Å, H₂N-NH₂: 1.453 Å),^{83,84} while angles around N8 and N9 suggest these atoms to be effectively sp² hybridized. Along these lines, free azide is isoelectronic with linear CO2, while the AdN₃ ligand in **3** is more in accord with bent NO₂-, implying a reduced azide functionality. Moreover, complex 3 displays a single N=N IR stretching mode (2088 cm⁻¹) at the low energy range for free AdN₃ (2142, 2086 cm⁻¹).⁴⁷ These structural and spectroscopic data suggest that 3, despite being tantalizingly labelled a formal Ti^{II} azide adduct {Ti-N=N=NAd}, might be best construed as a Ti^{IV} diazenylimide complex, {Ti≡N-N=NAd}. Computationally, natural population analysis reveals an electronic configuration more in line with a Ti^{III} center, which is further supported by strong π -backbonding between the metal center and the azide ligand (Figure S46).

Electronic Structure of a Titanium Azide Adduct (3)

Considering that **3** is the only known azide adduct of a divalent group 4 metal, we explored its electronic structure via density functional theory85 (DFT) calculations at the PBE-D3/cc-pVTZ(-f)/LACV3P//6-31G**/LACVP level of theory (See Supporting Information for details).86-91 In order to define a frame of reference, the imide complex 4 was first examined. It has a HOMO-1 and a HOMO that arise from bonding combinations of two orthogonal sets of atomic orbitals (N $2p_y/Ti 3d_{yz}$ and N $2p_x/Ti 3d_{xz}$), which are π -symmetric along the Ti≡N axis (Figure 2A). An analogous bonding picture emerges for the azide adduct 3, with the added complexity that the π -orbitals extend to N_{β} and N_{α} , and that there are one and two nodal plane(s) perpendicular to the N-N bonds, respectively, for the HOMO-1 and HOMO (Figure 2A). It is noteworthy that the HOMO of 3 carries the same number of nodal planes as the LUMO of CO₂ as well as the SOMO of NO₂, which supports an assignment of 3 as a diazenylimide complex, along with Ti≡N triple bond charac-

Returning to the higher energy frontier orbitals of 3, the LUMO essentially comprises a Ti $3d_{xy}$ orbital, as anticipated from oxo-wall considerations for tetragonal geometries. Still higher in energy lies the LUMO+1. This π^* MO consists of antibonding combinations of Ti $3d_{yz}/N$ $2p_y$ atomic orbitals, is energetically low-lying, and has considerable probability density on N_α and N_β . This foretells a possible π -backbonding capacity of 3, especially if assuming a configuration where the adamantyl group turns toward the $\{(Tp^{r_{Bu,Me}})TiCl\}$ platform to



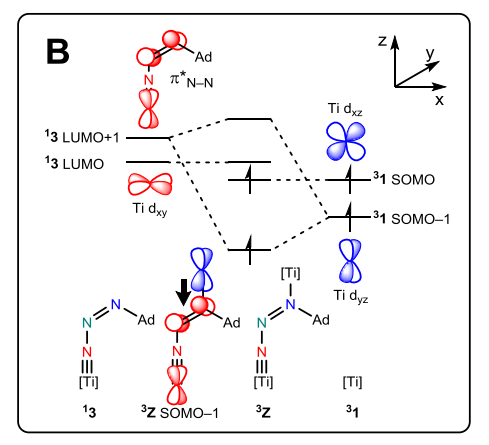


Figure 2. A: Conceptual molecular orbital diagrams for **3** and **4** (HOMO and HOMO–1). **B:** π -Acceptor propensity of **3**, illustrated for association with **1**.

accommodate an incoming metal center. Given the electron-rich nature of Ti^{II} complexes, a fragment such as $\mathbf{1}$ could π -backdonate to the α -N of the azide motif in $\mathbf{3}$ to form a putative dinuclear and paramagnetic species $[\{(Tp^{fBu,Me})TiCl\}(\alpha,\gamma;\mu\text{-N}_3Ad)\{(Tp^{fBu,Me})TiCl\}]$ (${}^3\mathbf{Z}$, Figure ${}^2\mathbf{B}$); the significance of such an interaction will be discussed below.

Deazotation of a Titanium Azide Adduct (3)

To obtain a quantitative understanding of the stability of 3, we studied its thermal conversion to 4. Having developed a protocol to access complex 3 in pure form from 1^{CNAd} or 2, we conducted kinetic studies. Deazotation could proceed in a number of ways (Chart 1B): Bergman^{52,53} and Chang⁵⁵ observed first-order decay of their Ta^{III} and V^{III} azide adducts; these reactions presumably proceed via $\{M(\alpha, y-N_3R)\}\$ intermediates or via intermittent formation of free nitrene, respectively. Contrarily, Cummins⁵⁴ used kinetic measurements and cross-over experiments to propose that their VIII azide adduct extrudes N2 in a second-order process. More recently, Hall used DFT methods to demonstrate that Abu-Omar's Re^V oxo complexes⁹² traverse {Re(α -N₃R)} adducts when converting to the corresponding ReVII oxo-imide products.^{59,60} Finally, Baik identified a {Zr(α,β-N₃R)} intermediate in nitrene transfer catalysis.⁶¹ In view of these distinct pathways, we studied the conversion of 3 to 4 by ¹H NMR spectroscopy, using Si(SiMe₃)₄ as an internal reference. Relative integrals from 3 (1.70 ppm, 3 ^tBu) and 4 (2.41 ppm, Ad) reaffirm a clean transformation, with no observable side products or intermediates in the remaining regions of the spectra (Figure 3A). Above room temperature, resonances from C_s symmetric 4 (Me, ^tBu) coalesce into broad features, the tails of which overlap with the sharp resonances from 3. At 70 °C, the decay was monitored at various initial concentrations of 3 and plotted on square root-, logarithmic- and inverse scales (Figure 3B). The square root and inverse plots yield clear curvature and dissimilar slopes, thus speaking against half- or second-order rate laws, respectively. On the other hand, the natural logarithm plot yields parallel straight lines, in accord with the transformation following a first-order rate law. Having thus established the decay of 3 to 4 to be unimolecular, we turned to temperature-dependent kinetic studies (50-90 °C). Within this temperature window, the half-life of 3 decreases from 43 h to 16 minutes (Figure 3C). Describing the corresponding rate constants by an Arrhenius law yields an activation energy of $E_a = 29(2)$ kcal mol⁻¹, and extrapolation from this simple model suggests a half-life of 61 days at 25 °C, in line with the considerable thermal stability of 3. Alternatively, an Eyring plot allows for the extraction of the activation parameters $\Delta H^{\ddagger} = 28(2)$ kcal mol⁻¹ and $\Delta S^{\ddagger} = 4.9(5.3)$ cal mol⁻¹ K⁻¹ (inset in **Figure 3C**); this essentially shows **3** to have a relatively high energetic barrier for deazotation, which varies only slightly with temperature. Considering the standard uncertainty, the activation entropy is quite close to zero, suggesting a fairly ordered transition state, consistent with deazotation proceeding in a unimolecular fashion.

In view of the array of conceivable unimolecular deazotation pathways available to azide adducts (Chart 1B), we

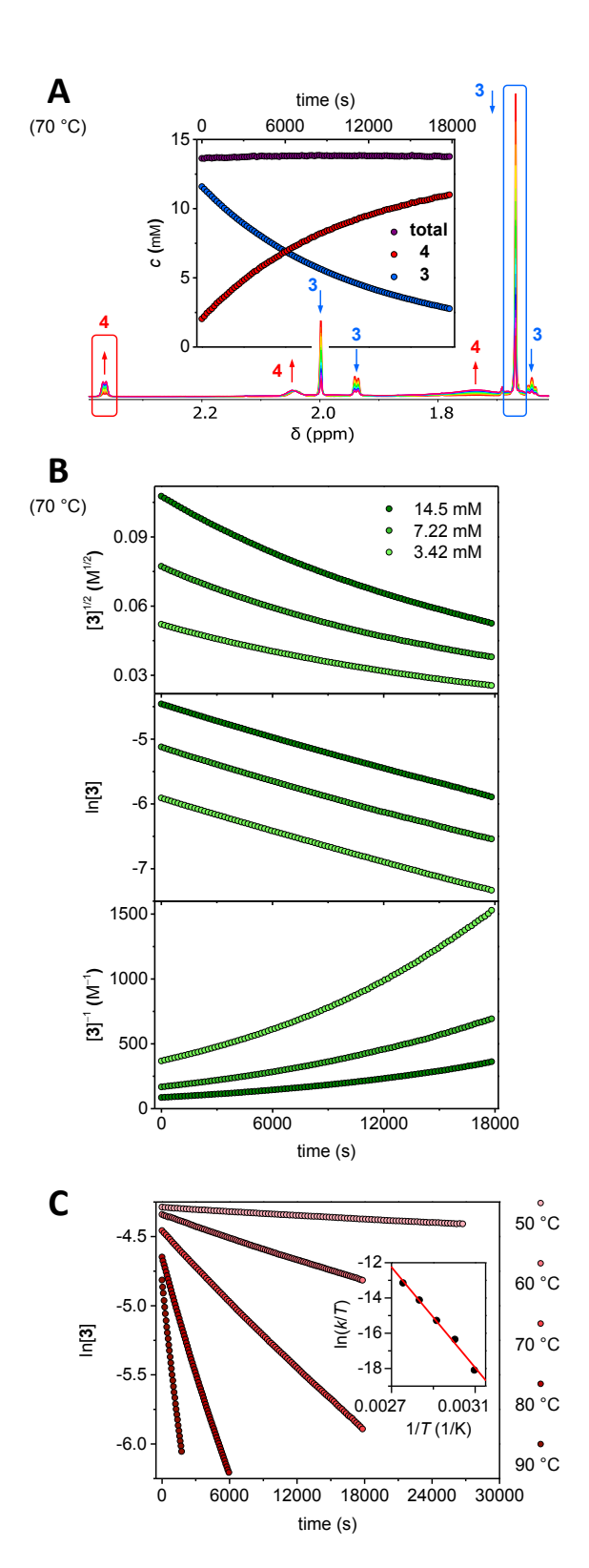


Figure 3. Kinetic studies of the conversion of **3** to **4** in C₆D₆. **A:** Concentration of **3** and **4** determined from ¹H NMR spectroscopy. **B:** Square root, natural logarithm, and inverse of [**3**] *versus* time (each with three different concentrations at 70 °C). **C:** Temperature dependence of ln[**3**] *versus* time (50–90 °C) along with an Eyring plot (inset).

gathered further mechanistic information using DFT. All intermediates considered are, by necessity, isomers of 3 and therefore denoted by those nitrogen atoms of AdN₃ that coordinate to Ti. Four distinct pathways were examined. First, the formation of an analog of Hall's $\{Re(\alpha-N_3R)\}$ intermediate would commence with dissociation of AdN₃ from 3. Although a transition state was not identified, the microscopic reverse of this process has a thermodynamic driving force of 33.7 kcal mol⁻¹ (vide infra, **Figure 7**), which well surpasses the experimental barrier for deazotation. Second, Hillhouse's isolation of $\{Ni(\beta, \gamma-N_3R)\}\$ adducts⁴⁹⁻⁵¹ coupled with the viability of Baik's $\{Zr(\alpha,\beta-N_3R)\}$ computed intermediate, 61 suggests that N₂ extrusion could occur via initial slippage of the azide ligand to generate n2-N3Ad isomers of 3 (Figure 4, red dashed line). In fact, this leads to a $[(Tp^{t_{Bu,Me}})TiCl(\beta, v-N_3Ad)]$ intermediate $(3^{\beta,\gamma})$ at slightly higher energy than 3 (7.0 kcal mol-1). However, the following transition state $(3^{\beta,\gamma}$ -TS), where all N atoms of the azide ligand interact with Ti before slipping to an α,β -coordination mode, has a prohibitively high energetic barrier (41.1) kcal mol-1) when compared to experiment. Third, Bergman suggested that hydrocarbyl migration from N_{α} to N_{γ} could generate, in our case, a $[(Tp^{t_{Bu,Me}})TiCl(\alpha-N_3Ad)]$ intermediate (3^{α}) poised for N_2 extrusion (**Figure 4**, red solid line). Unsurprisingly, the computed barrier for the accompanying transition state is practically insurmountable (3'-TS, >120 kcal mol-1). Finally, Bergman identified a cyclization pathway as a plausible mechanistic scenario. This process traverses two transition states (3-TS and $3^{\alpha,\gamma}$ -TS, Figure 4, black line); the first involves bond formation between Ti and N_{α} , leading to a titanatriazete intermediate [(Tp^{tBu,Me})TiCl(α , γ -N₃Ad)] ($3^{\alpha,\gamma}$). Strong σ - and π -donation from the formal organoazide dianion to the Ti^{IV} center aids the formation of the titanacycle, thus compensating for the severe structural distortion of the azide moiety (Figure

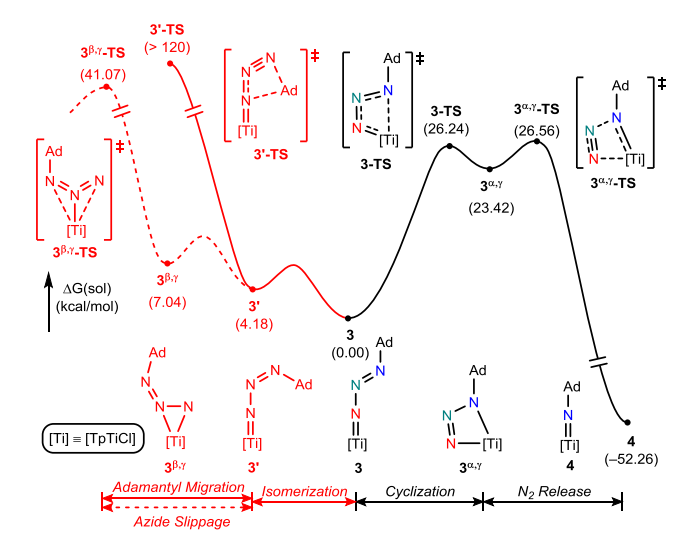


Figure 4. Relative Gibbs free energy diagram leading from **3** to **4**. Red dashed line: Pathway via azide slippage. Red solid line: Pathway via adamantyl migration. Black line: Pathway via cyclization into a titanatriazete intermediate. T = 343.15 K.

S47). The activation barrier for this step is likely rate determining (26.6 kcal mol⁻¹) and numerically very close to the experimental activation Gibbs free energy ($\Delta G^{\dagger}_{343K} = 26(3)$ kcal mol⁻¹). Subsequently, [2+2]-retrocycloaddition of N₂ leads to 4, which is the sole product resulting from deazotation of 3. The overall transformation of 3 to 4 is highly exergonic (-52.3 kcal mol-1) and only slightly perturbed by temperature changes, in line with the experimental value for ΔS^{\ddagger} being close to zero (within experimental uncertainty, vide supra). We also evaluated the cyclization pathway in terms of steric constraints imposed by the Tp^{tBu,Me} ligand (Figure S48). Upon reducing the substituent size (^tBu replaced by Me), the activation barrier for deazotation decreases from 26.6 kcal mol⁻¹ to 8.0 kcal mol⁻¹, suggesting the stability of azide adduct 3 to largely originate in steric repulsion between the ^tBu and Ad groups. Along these lines, the direct transformation of 1 and Me₃SiN₃ into [(Tp^{tBu,Me})TiCl(NSiMe₃)] in preference to the hypothetical azide adduct, "[$(Tp^{tBu,Me})TiCl(\gamma-N_3SiMe_3)$]",64 is most likely rooted in sterics.

Association of AdN₃ with a Titanium Dinitrogen Complex (2)

To examine the origin of the selectivity difference in reactions of AdN_3 toward Ti^{II} complex ${\bf 1}$ on the one hand, and dinitrogen adduct ${\bf 2}$ (or ${\bf 1}^{CNAd}$) on the other hand, we turned to computational studies. First focusing on the dinitrogen complex, we initially notice that dissociation of diamagnetic ${\bf 2}$ into ${\bf 1}$ and a triplet N_2 complex, $[(Tp^{\ell Bu,Me})TiCl(N_2)]$ (${\bf 3Y}$),

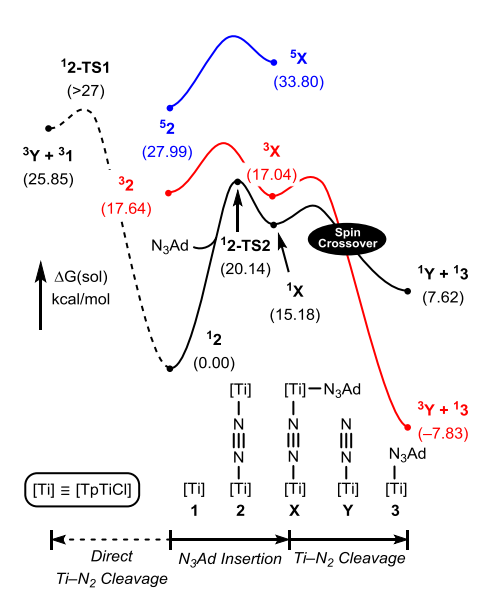
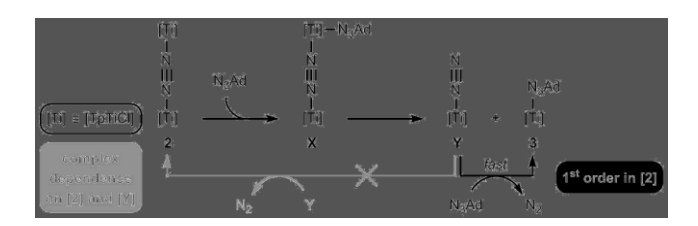


Figure 5. Proposed pathway for the conversion of $\bf 2$ with AdN₃ to generate $\bf 3$. T = 343.15 K.

requires more than 27 kcal mol⁻¹, which is comparable to the energetic barrier for deazotation of **3** into **4**, and thus unlikely (**Figure 5**, black dashed line). A lower energy pathway commences with association between AdN₃ and one of the Ti centers in **2** to generate a N₂-bridged azide adduct $[\{(Tp^{tBu,Me})TiCl\}(\mu-N_2)\{(Tp^{tBu,Me})TiCl(\gamma-N_3Ad)\}]$ (¹X; **Figure**

5, black solid line). An energetic barrier of 20.1 kcal mol⁻¹ accompanies this process, rendering it likely rate determining. Spin crossover and fragmentation of ¹X leads to 3 along with ³Y (Figure 5, red/black solid lines). From ³Y, two mechanistic pathways could conceivably be operative. The first involves direct association between AdN3 and 3Y to generate 3 and N2, whereas the second involves recombination between two equivalents of ³Y to generate 2 and one equivalent of N₂ (Scheme 2). To experimentally discern the two possible pathways, we probed the conversion of 2 with excess AdN₃ by ¹H NMR spectroscopy (as outlined previously). Between 15-45 °C, complex 2 converts to 3 (and minor amounts of 4; ca. 5% at 45 °C); no intermediates or sideproducts were observable. Inspection of the time dependence of the square root, logarithmic and inverse concentrations of [2] (normalized by a constant corresponding to [AdN₃]), suggests a first-order dependence on [2] in preference to half- or second-order dependencies (Figure 6A). Moreover, the observed pseudo first-order rate constants (k_{obs}) scale linearly with [AdN₃], in line with an overall second-order rate law ($v = k_2 \cdot [2] \cdot [AdN_3]$, *cf.* inset in **Figure 6B**). Finally, temperature-dependent studies (Figure 6C) yielded a set of 2nd-order rate constants, which could be described by a simple Arrhenius law to yield an activation energy of $E_a = 24(1)$ kcal mol⁻¹, whereas an Eyring plot yielded activation parameters of ΔH^{\ddagger} = 23(1) kcal mol⁻¹ and ΔS^{\ddagger} = 7.2(4.3) cal mol⁻¹ K⁻¹. The computed barrier (20.1 kcal mol⁻ ¹, black trace in **Figure 5**) is in excellent agreement with the experimental activation Gibbs free energy ($\Delta G^{\dagger}_{343K} = 21(2)$) kcal mol⁻¹). When comparing the conversion of **2** to **3** to the conversion of 3 to 4, there is a notable increase in the experimental and theoretical values for E_a and $\Delta G^{\dagger}_{343K}$ (all on the order of +5 kcal mol⁻¹), in line with the metastable nature of



Scheme 2. Mechanistic scenarios for the reaction between **2** and AdN_3 , leading to **3**. Black path: Intermediate **Y** reacts directly with AdN_3 to generate **3** and N_2 . Gray path: Two units of intermediate **Y** recombine to generate **2** and N_2 .

the azide adduct. Returning to **Figure 5** and **Scheme 2**, the kinetically observed first-order dependence on [2] suggests intermediate ${}^3\mathbf{Y}$ to associate with $\mathrm{AdN_3}$ in preference to regenerating **2**, as the latter scenario necessitates a more complex rate law depending on both [2] and [Y]. This might be anticipated based on the relatively large initial concentration of $\mathrm{AdN_3}$ (46–330 mM) as compared to **2** (2–8 mM); given the relatively slow progress of the reaction, intermediate ${}^3\mathbf{Y}$ must be present in even lower concentrations.

Reactivity of AdN₃ Toward a Tetrahedral Ti^{II} Complex (1)

Having examined how AdN_3 selectively transforms $\bf 2$ to $\bf 3$, we went on to address why AdN_3 instead transforms $\bf 1$ to a mixture of $\bf 3$ and $\bf 4$. The simplest explanation would be that AdN_3 either associates with the coordinatively unsaturated

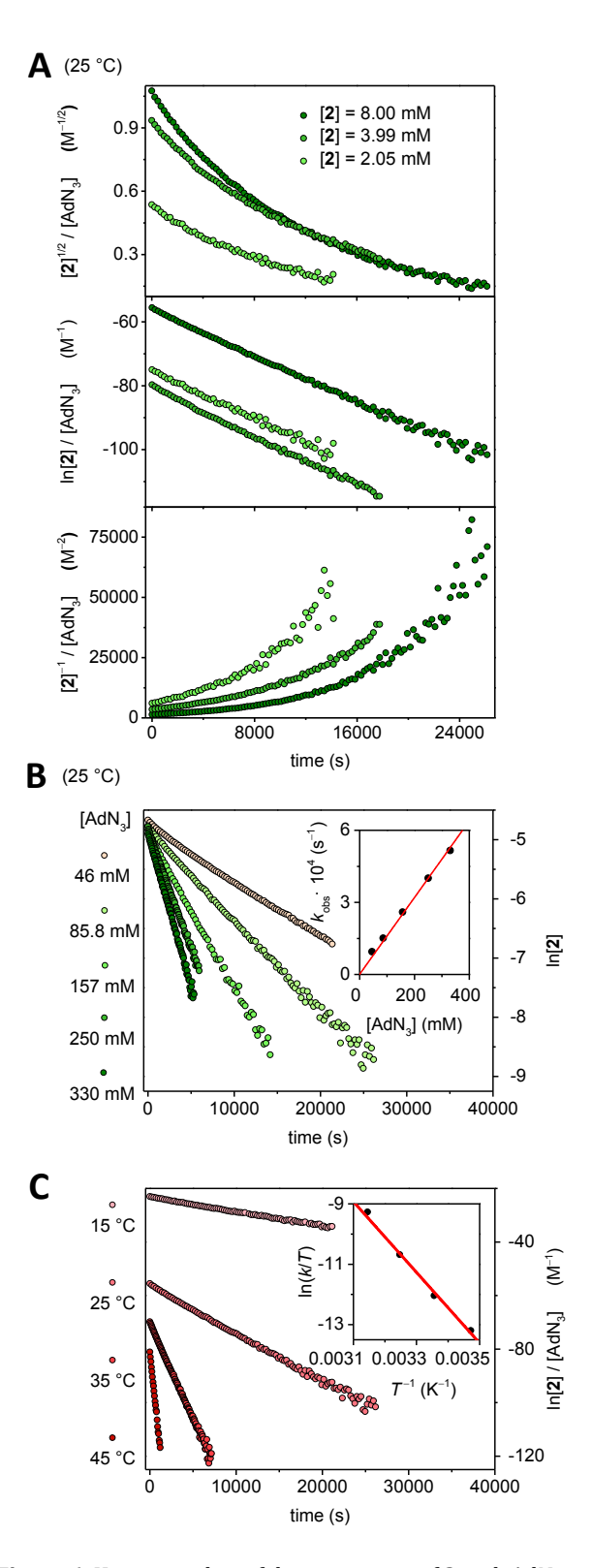
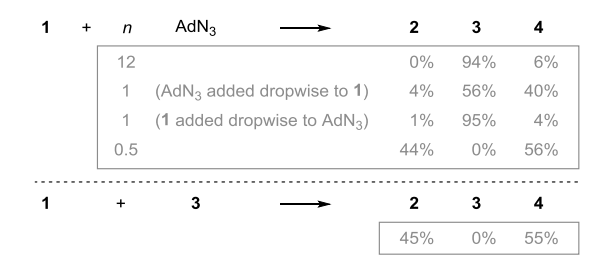


Figure 6. Kinetic studies of the conversion of **2** with AdN_3 to generate **3** in C_6D_6 . **A:** Square root, natural logarithm, and inverse of [**2**] *versus* time (three concentrations, normalized by [AdN₃]). **B:** Dependence of $\ln[\mathbf{2}]$ *versus* time as well as k_{obs} (inset) on [AdN₃]. **C:** Temperature dependence of $\ln[\mathbf{2}]$ · [AdN₃]⁻¹ *versus* time (15–45 °C) along with an Eyring plot (inset).

Ti^{II} center through N_{γ} to afford the stable azide adduct 3, whereas association through N_{α} would yield an isomer, [(Tp^{'Bu,Me})TiCl(α -N₃Ad)] (3°), which is poised for N₂ extrusion. Computationally, it was found that 3° is highly unstable, with geometry optimizations proceeding directly to N₂ and 4. Notably, the product distribution would be invariant with respect to reactant concentration if the relative orientation between metal and azide determined which product would form on the molecular level. To experimentally evaluate competing N_{\alpha} and N_{\gamma} coordination, dropwise addition of a toluene solution of AdN₃ to a solution containing one equivalent of 1 under argon afforded comparable amounts of 3 (56%) and 4 (40%) along with trace 2 (4%) within



Scheme 3. Product distributions resulting upon treatment of 1 with 12, 1, or 0.5 equivalents of AdN_3 (top) or with 1 equivalent of 3 (bottom).

minutes (**Scheme 3**). [Note that spectroscopic yields involving **2** are based on relative integrals (rather than relative concentrations) in order to simplify comparisons between mono- and bimetallic complexes]. However, reversing the order of addition, i.e. by adding a solution of **1** dropwise to a solution containing one equivalent of AdN₃, resulted in a completely different product distribution favoring the azide adduct: **2** (1%), **3** (95%), **4** (4%). Likewise, quick addition of a 12-fold molar excess of AdN₃ to **1** generated but trace amounts of imide **4** (6%), whereas the azide adduct **3** (94%) became the dominant product, thus speaking against competing N_{α}/N_{γ} coordination of AdN₃ (**Scheme 3**).

Given the π -backbonding capabilities of 3 (vide supra, **Fig**ure 2B), we considered this molecule as an intermediate en route to 4 (Figure 7). Initially, coordination of AdN₃ to 1 is energetically favored by 33.7 kcal mol⁻¹. The equivalent of 3 formed in this way adopts a cis-configuration around the diazenyl unit, allowing for association with free $\mathbf{1}$ via N_{α} ; this affords bimetallic triplet intermediate, [$\{(Tp^{tBu,Me})TiCl\}(\alpha,\gamma;\mu-N_3Ad)\{(Tp^{tBu,Me})TiCl\}\}$ (3**Z**), which lies 4.9 kcal mol⁻¹ lower in energy than **3**. Importantly, the π backbonding interaction activates the N_{α} - N_{β} bond toward scission. Thus, ³Z traverses a modest energetic barrier (9.6 kcal mol-1) accompanying transition state 3Z-TS, before fragmenting into 4 and the N₂-intermediate, ³Y. Kinetic data from the conversion of 2 with AdN₃ (Figure 6) suggest that intermediate ³Y then reacts with AdN₃ to regenerate 3. Consequently, the formation of 4 only continues as long as unconverted **1** is available. This pathway is consistent with the product distributions observed in reactions of 1 with equimolar or excess AdN₃ and also explains the different product distributions observed when the order of addition is changed (metal complex to azide versus the reverse, **Scheme 3**). Generally speaking, an excess of AdN₃ would deplete **1** before ³**Z** could build up, thus favoring azide adduct **3** over imide complex **4**. To further probe the proposed pathway, treatment of **1** with 0.5 eq. of AdN₃ cleanly af-

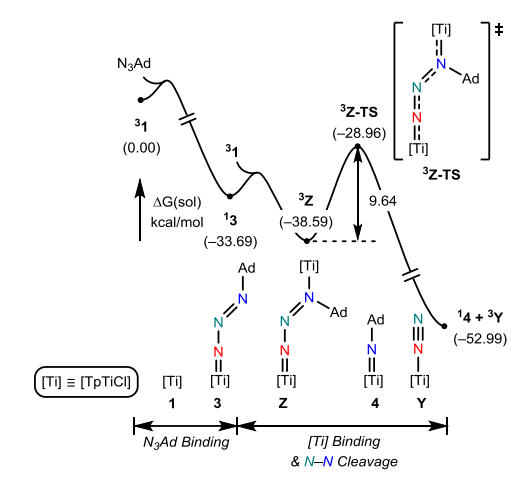


Figure 7. Proposed pathway for the conversion of **1** with AdN_3 into **3** followed by the formation of a bimetallic triplet intermediate ${}^3\mathbf{Z}$, which finally releases **4**. T = 343.15 K.

forded imide complex 4 (56%) and dinitrogen complex 2 (44%) without observable amounts of azide adduct 3, in accord with the formation and subsequent fracture of an intermediate akin to ³Z. The most compelling indication of a bimetallic mono-azide intermediate comes from the direct reaction between isolated samples of 1 and 3 (Schemes 1, 3). This reaction cleanly furnishes 4 (55%) and 2 (45%) within minutes, confirming 3 to be a competent intermediate in bimolecular deazotation reactions starting from 1. As expected, ¹H NMR spectra of **1** treated with 0.5 eq. of AdN₃ or with 1 eq. of 3 are essentially superimposable. Finally, the observation that AdN₃ cleanly transforms 1^{CNAd} to 3 without proceeding to 4 (Scheme 1) suggests that the isocyanide ligand in 1^{CNAd} blocks the Ti^{II} center, thus preventing the assembly of a reactive bimetallic mono-azide adduct akin to 3Z.

To illustrate the stability of organoazide adducts across the periodic table, particularly keeping the historic importance of vanadium in mind, 54,55 we inquired whether the V^{II} analog of 1, [(Tp^{tBu,Me})VCl] (1^V),⁸¹ might transform to a paramagnetic azide adduct. In this context, it is notable that the formal d^5 and d^8 systems, $[\{(Tp^{tBu,Me})M\}_2(\mu-N_2)]$ (M = Cr. 10 Co⁴), directly convert to imide complexes upon exposure to AdN₃. By contrast, no reaction occurs between 1^v and AdN₃ at room temperature (¹H NMR), and neither does 1^v react with 3. However, irradiation of a reaction mixture of **1**^v and AdN₃ (full spectrum from a Xe lamp over 3 hours) generated a green paramagnetic product. Crystallographic characterization revealed $[(Tp^{tBu,Me})VCl(NC_{10}H_{15})]$ (5, $\tau_5 = 0.27$), bearing "NAd" in the form of a bicyclic imine ligand resulting from ring-expansion via nitrene insertion into an adamantyl C-C bond (Fig**ure 8**). The solubility of **5** is similar to that of the organic starting material/byproducts, hampering isolation of a pure product. Typically, **5** was isolated in ca. 30% yield but the d^3 system co-crystallizes with organic byproducts. Regardless,

in its free state, the bicyclic imine, 4-azahomoadamant-3-ene, dimerizes in a [2+2] cycloaddition. $^{93-95}$ Dias 44 and Powers 47 recently used late transition metal fragments such as Au^I or Rh^{II} to confer stability upon the imine. Conceivably, coordination to the early transition metal, V^{II} , could enable useful derivatizations of the bicyclic imine, but most importantly, the divergent reactivity between 1, 1^V , and the related bimetallic N_2 -complexes of Cr^I/Co^I highlights the delicate role of the metal ion in stabilizing organoazide adducts: The metal must activate the azide moiety sufficiently to promote coordination, albeit not to an extent where N_2 extrusion commences.

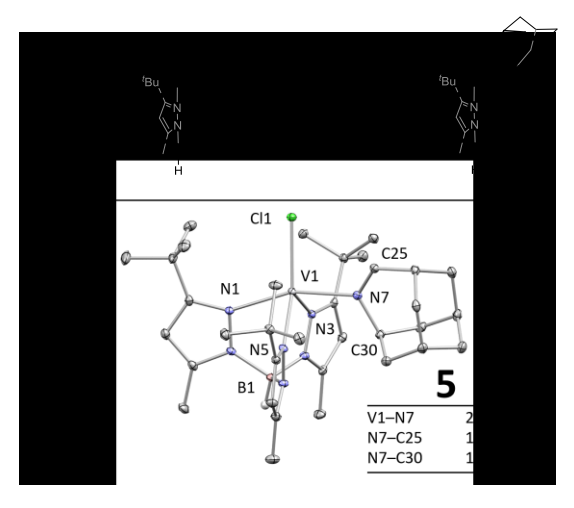


Figure 8. A: Photolytic conversion of $\mathbf{1}^{\mathbf{v}}$ and AdN_3 into imine complex **5. B:** Thermal ellipsoid plot of **5** (50% probability).

CONCLUSIONS

In summary, a tetrahedral Ti^{II} complex 1 reacts with AdN₃ to concurrently generate an imide complex (4) and a hitherto unknown mononuclear azide adduct of a group 4 transition metal, 3. The product distribution depends critically on relative concentrations: An excess of 1 favors imide complex 4, whereas an excess of AdN3 favors azide adduct 3; even the order in which the reactants are combined suffices to determine which product forms. Complex 3 also forms in high yield upon treating π -acid adducts of 1 (1^{CNAd}, 2) with AdN₃. The thermal conversion of 3 to 4 follows unimolecular kinetics, has an activation entropy close to zero, and proceeds through a titanatriazete intermediate. Yet, the conversion is characterized by a substantial kinetic barrier ($t_{\frac{1}{2}}$ = 61 days at 25 °C), which fails to explain the parallel formation of 3 and 4 in direct reactions between 1 and AdN₃ at room temperature. Along these lines, π -acceptor character enables azide adduct 3 to associate with free Ti^{II} complex 1, thus forming a more reactive bimetallic mono-azide intermediate, 3Z. As for practical implications of this study, we note that transition metal azide adducts that follow bifurcated deazotation pathways are remarkably rare, while bimetallic mono-azide intermediates akin to 3Z have not been invoked nor recognized heretofore despite organoazide to imide conversion being a well-known transformation. These unconventional intermediates are relevant to deazotation reactions that display crossover⁵⁴ or require sub-stoichiometric azide.⁴⁹ In a broader perspective, it is notable

that metastable azide adducts might exert a yet unappreciated retarding effect in nitrene transfer catalysis, particularly given the typical employment of excess nitrene source. The order of reactant addition also plays a significant role in the observation of otherwise undetected intermediates.

ASSOCIATED CONTENT

Supporting Information

Synthetic procedures; NMR, IR, UV-vis, kinetic, and computational data. This material is available free of charge via the Internet at http://pubs.acs.org.

Accession codes

CCDC 2116923–2116926 contain the supplementary crystallographic data for this paper. These data can be obtained free of charge via www.ccdc.cam.ac.uk/data_request/cif, or by emailing data_request@ccdc.cam.ac.uk, or by contacting The Cambridge Crystallographic DataCentre, 12 Union Road, Cambridge CB2 1EZ, UK; fax: +44 1223 336033.

AUTHOR INFORMATION

Corresponding Authors

*Mu-Hyun Baik	ORCID: 0000-0002-8832-8187
	mbaik2805@kaist.ac.kr
*Daniel J. Mindiola	ORCID: 0000-0001-8205-7868
	mindiola@sas.upenn.edu

Authors

Seongyeon Kwon ORCID: 0000-0002-374 Mehrafshan G. Jafari ORCID: 0000-0001-680 Michael R. Gau ORCID: 0000-0002-479 Patrick J. Carroll ORCID: 0000-0002-814 Chad Lawrence ORCID: 0000-0001-694 Iun Gu: ORCID: 0000-0003-270	07-7520 90-6980 42-7211 46-6982
Jun Gu: ORCID: 0000-0003-270)1-4421

Author Contributions

The manuscript was written through contributions of all authors. All authors have given approval to the final version of the manuscript. ‡These authors contributed equally.

Notes

The authors declare no competing financial interest.

ACKNOWLEDGMENT

A.R. gratefully acknowledges The Carlsberg Foundation (Grant CF18-0613) and the Independent Research Fund Denmark (Grant 9036-00015B) for funding. We thank the U.S. National Science Foundation (NSF; CHE-1464659) and the University of Pennsylvania for funding. We thank the Institute for Basic Science in Korea for financial support (IBS-R010-A1).

ABBREVIATIONS

Ad = 1-adamantyl, 'Bu: *tert*-butyl, Cp: cyclopentadienyl, Cp* pentamethylcyclopentadienyl, Me: methyl, Ph: phenyl.

REFERENCES

- Jenkins, D. M.; Betley, T. A.; Peters, J. C., Oxidative Group Transfer to Co(I) Affords a Terminal Co(III) Imido Complex. J. Am. Chem. Soc. 2002, 124, 11238-11239.
- Betley, T. A.; Peters, J. C., Dinitrogen Chemistry from Trigonally Coordinated Iron and Cobalt Platforms. J. Am. Chem. Soc. 2003, 125, 10782-10783.

- Hu, X.; Meyer, K., Terminal Cobalt(III) Imido Complexes Supported by Tris(Carbene) Ligands: Imido Insertion into the Cobalt-Carbene Bond. J. Am. Chem. Soc. 2004, 126, 16322-16323.
- Shay, D. T.; Yap, G. P. A.; Zakharov, L. N.; Rheingold, A. L.; Theopold, K. H., Intramolecular C-H Activation by an Open-Shell Cobalt(III) Imido Complex. *Angew. Chem., Int. Ed.* 2005, 44, 1508-1510.
- King, E. R.; Sazama, G. T.; Betley, T. A., Co(III) Imidos Exhibiting Spin Crossover and C-H Bond Activation. J. Am. Chem. Soc. 2012, 134, 17858-17861.
- Wu, B.; Hernández Sánchez, R.; Bezpalko, M. W.; Foxman, B. M.; Thomas, C. M., Formation of Heterobimetallic Zirconium/Cobalt Diimido Complexes via a Four-Electron Transformation. *Inorg. Chem.* 2014, 53, 10021-10023.
- Geer, A. M.; Tejel, C.; López, J. A.; Ciriano, M. A., Terminal Imido Rhodium Complexes. *Angew. Chem., Int. Ed.* 2014, 53, 5614-5618.
- Zhang, L.; Liu, Y.; Deng, L., Three-Coordinate Cobalt(IV) and Cobalt(V) Imido Complexes with N-Heterocyclic Carbene Ligation: Synthesis, Structure, and Their Distinct Reactivity in C-H Bond Amination. J. Am. Chem. Soc. 2014, 136, 15525-15528.
- Du, J.; Wang, L.; Xie, M.; Deng, L., A Two-Coordinate Cobalt(II) Imido Complex with NHC Ligation: Synthesis, Structure, and Reactivity. Angew. Chem., Int. Ed. 2015, 54, 12640-12644.
- Akturk, E. S.; Yap, G. P. A.; Theopold, K. H., Mechanism-based design of labile precursors for chromium(I) chemistry. *Chem. Commun.* 2015, 51, 15402-15405.
- 11. Liu, Y.; Du, J.; Deng, L., Synthesis, Structure, and Reactivity of Low-Spin Cobalt(II) Imido Complexes [(Me₃P)₃Co(NAr)]. *Inorg. Chem.* **2017**, *56*, 8278-8286.
- Yao, X.-N.; Du, J.-Z.; Zhang, Y.-Q.; Leng, X.-B.; Yang, M.-W.; Jiang, S.-D.; Wang, Z.-X.; Ouyang, Z.-W.; Deng, L.; Wang, B.-W.; Gao, S., Two-Coordinate Co(II) Imido Complexes as Outstanding Single-Molecule Magnets. J. Am. Chem. Soc. 2017, 139, 373-380.
- Aldrich, K. E.; Odom, A. L., A photochemical route to a square planar, ruthenium(IV)-bis(imide). *Chem. Commun.* 2019, 13, 4403-4406.
- Martinez, J. L.; Lutz, S. A.; Yang, H.; Xie, J.; Telser, J.; Hoffman, B. M.; Carta, V.; Pink, M.; Losovyj, Y.; Smith, J. M., Structural and spectroscopic characterization of an Fe(VI) bis(imido) complex. *Science* 2020, 370, 356-359.
- Mankad, N. P.; Müller, P.; Peters, J. C., Catalytic N-N Coupling of Aryl Azides To Yield Azoarenes via Trigonal Bipyramid Iron-Nitrene Intermediates. J. Am. Chem. Soc. 2010, 132, 4083-4085.
- 16. Takaoka, A.; Moret, M.-E.; Peters, J. C., A Ru(I) Metalloradical That Catalyzes Nitrene Coupling to Azoarenes from Arylazides. *J. Am. Chem. Soc.* **2012**, *134*, 6695-6706.
- 17. Nguyen, A. I.; Zarkesh, R. A.; Lacy, D. C.; Thorson, M. K.; Heyduk, A. F., Catalytic nitrene transfer by a zirconium(IV) redox-active ligand complex. *Chem. Sci.* **2011**, *2*, 166-169.
- Kriegel, B. M.; Bergman, R. G.; Arnold, J., Nitrene Metathesis and Catalytic Nitrene Transfer Promoted by Niobium Bis(imido) Complexes. J. Am. Chem. Soc. 2016, 138, 52-55.
- Gao, G.-Y.; Jones, J. E.; Vyas, R.; Harden, J. D.; Zhang, X. P., Cobalt-Catalyzed Aziridination with Diphenylphosphoryl Azide (DPPA): Direct Synthesis of *N*-Phosphorus-Substituted Aziridines from Alkenes. *J. Org. Chem.* 2006, 71, 6655-6658.
- Cramer, S. A.; Jenkins, D. M., Synthesis of Aziridines from Alkenes and Aryl Azides with a Reusable Macrocyclic Tetracarbene Iron Catalyst. J. Am. Chem. Soc. 2011, 133, 19342-19345.
- Cramer, S. A.; Hernández Sánchez, R.; Brakhage, D. F.; Jenkins,
 D. M., Probing the role of an Fe^{IV} tetrazene in catalytic aziridination. *Chem. Commun.* 2014, 50, 13967-13970.
- Gilbert, Z. W.; Hue, R. J.; Tonks, I. A., Catalytic formal [2+2+1] synthesis of pyrroles from alkynes and diazenes via Ti^{II}/Ti^{IV} redox catalysis. *Nat. Chem.* 2016, 8, 63-68.

- Davis-Gilbert, Z. W.; Yao, L. J.; Tonks, I. A., Ti-Catalyzed Multicomponent Oxidative Carboamination of Alkynes with Alkenes and Diazenes. J. Am. Chem. Soc. 2016, 138, 14570-14573.
- 24. Pearce, A. J.; See, X. Y.; Tonks, I. A., Oxidative nitrene transfer from azides to alkynes via Ti(II)/Ti(IV) redox catalysis: formal [2+2+1] synthesis of pyrroles. *Chem. Commun.* **2018**, *54*, 6891-6894.
- Hennessy, E. T.; Betley, T. A., Complex N-Heterocycle Synthesis via Iron-Catalyzed, Direct C–H Bond Amination. *Science* 2013, 340, 591-595.
- Hennessy, E. T.; Liu, R. Y.; Iovan, D. A.; Duncan, R. A.; Betley, T. A., Iron-mediated intermolecular N-group transfer chemistry with olefinic substrates. *Chem. Sci.* 2014, 5, 1526-1532.
- Iovan, D. A.; Wilding, M. J. T.; Baek, Y.; Hennessy, E. T.; Betley, T. A., Diastereoselective C-H Bond Amination for Disubstituted Pyrrolidines. *Angew. Chem., Int. Ed.* 2017, 56, 15599-15602.
- Baek, Y.; Betley, T. A., Catalytic C-H Amination Mediated by Dipyrrin Cobalt Imidos. J. Am. Chem. Soc. 2019, 141, 7797-7806
- Baek, Y.; Hennessy, E. T.; Betley, T. A., Direct Manipulation of Metal Imido Geometry: Key Principles to Enhance C-H Amination Efficacy. J. Am. Chem. Soc. 2019, 141, 16944-16953.
- 30. Baek, Y.; Das, A.; Zheng, S.-L.; Reibenspies, J. H.; Powers, D. C.; Betley, T. A., C–H Amination Mediated by Cobalt Organoazide Adducts and the Corresponding Cobalt Nitrenoid Intermediates. *J. Am. Chem. Soc.* **2020**, *142*, 11232-11243.
- 31. Dong, Y.; Clarke, R. M.; Porter, G. J.; Betley, T. A., Efficient C-H Amination Catalysis Using Nickel-Dipyrrin Complexes. *J. Am. Chem. Soc.* **2020**, *142*, 10996-11005.
- Dong, Y.; Lund, C. J.; Porter, G. J.; Clarke, R. M.; Zheng, S.-L.; Cundari, T. R.; Betley, T. A., Enantioselective C-H Amination Catalyzed by Nickel Iminyl Complexes Supported by Anionic Bisoxazoline (BOX) Ligands. J. Am. Chem. Soc. 2021, 143, 817-829
- 33. Ballhausen, C. J.; Gray, H. B., The Electronic Structure of the Vanadyl Ion. *Inorg. Chem.* **1962**, *1*, 111-122.
- 34. Winkler, J. R.; Gray, H. B., Electronic Structures of Oxo-Metal Ions. In *Molecular Electronic Structures of Transition Metal Complexes I*, Mingos, D. M. P.; Day, P.; Dahl, J. P., Eds. Springer Berlin Heidelberg: Berlin, Heidelberg, 2012; pp 17-28.
- 35. Larson, V. A.; Battistella, B.; Ray, K.; Lehnert, N.; Nam, W., Iron and Manganese Oxo Complexes, Oxo Wall and Beyond. *Nat. Rev. Chem.* **2020**, *4*, 404-419.
- Barz, M.; Herdtweck, E.; Thiel, W. R., Transition Metal Complexes with Organoazide Ligands: Synthesis, Structural Chemistry, and Reactivity. *Angew. Chem., Int. Ed.* 1998, 37, 2262-2265.
- 37. Dias, H. V. R.; Polach, S. A.; Goh, S.-K.; Archibong, E. F.; Marynick, D. S., Copper and Silver Complexes Containing Organic Azide Ligands: Syntheses, Structures, and Theoretical Investigation of [HB(3,5-(CF₃)₂Pz)₃]CuNNN(1-Ad) and [HB(3,5-(CF₃)₂Pz)₃]AgN(1-Ad)NN (Where Pz = Pyrazolyl and 1-Ad = 1-Adamantyl). *Inorg. Chem.* 2000, *39*, 3894-3901.
- Albertin, G.; Antoniutti, S.; Baldan, D.; Castro, J.; García-Fontán, S., Preparation of Benzyl Azide Complexes of Iridium(III). *Inorg. Chem.* 2008, 47, 742-748.
- Brotherton, W. S.; Michaels, H. A.; Simmons, J. T.; Clark, R. J.;
 Dalal, N. S.; Zhu, L., Apparent Copper(II)-Accelerated Azide–Alkyne Cycloaddition. *Org. Lett.* 2009, 11, 4954-4957.
- Kuang, G.-C.; Michaels, H. A.; Simmons, J. T.; Clark, R. J.; Zhu, L., Chelation-Assisted, Copper(II)-Acetate-Accelerated Azide– Alkyne Cycloaddition. J. Org. Chem. 2010, 75, 6540-6548.
- 41. Allão, R. A.; Jordão, A. K.; Resende, J. A. L. C.; Cunha, A. C.; Ferreira, V. F.; Novak, M. A.; Sangregorio, C.; Sorace, L.; Vaz, M. G. F., Determination of the relevant magnetic interactions in low-dimensional molecular materials: the fundamental role of single crystal high frequency EPR. *Dalton Trans.* 2011, 40, 10843-10850.

- 42. Brotherton, W. S.; Guha, P. M.; Phan, H.; Clark, R. J.; Shatruk, M.; Zhu, L., Tridentate complexes of 2,6-bis(4-substituted-1,2,3-triazol-1-ylmethyl)pyridine and its organic azide precursors: an application of the copper(II) acetate-accelerated azide-alkyne cycloaddition. *Dalton Trans.* 2011, 40, 3655-3665.
- 43. Yuan, Z.; Kuang, G.-C.; Clark, R. J.; Zhu, L., Chemoselective Sequential "Click" Ligation Using Unsymmetrical Bisazides. *Org. Lett.* **2012**, *14*, 2590-2593.
- 44. Dash, C.; Yousufuddin, M.; Cundari, T. R.; Dias, H. V. R., Gold-Mediated Expulsion of Dinitrogen from Organic Azides. *J. Am. Chem. Soc.* **2013**, *135*, 15479-15488.
- Grant, L. N.; Carroll, M. E.; Carroll, P. J.; Mindiola, D. J., An Unusual Cobalt Azide Adduct That Produces a Nitrene Species for Carbon–Hydrogen Insertion Chemistry. *Inorg. Chem.* 2016, 55, 7997-8002.
- Vaddypally, S.; McKendry, I. G.; Tomlinson, W.; Hooper, J. P.; Zdilla, M. J., Electronic Structure of Manganese Complexes of the Redox-Non-innocent Tetrazene Ligand and Evidence for the Metal-Azide/Imido Cycloaddition Intermediate. *Chem. Eur.* J. 2016, 22, 10548-10557.
- 47. Das, A.; Chen, Y.-S.; Reibenspies, J. H.; Powers, D. C., Characterization of a Reactive Rh₂ Nitrenoid by Crystalline Matrix Isolation. *J. Am. Chem. Soc.* **2019**, *141*, 16232-16236.
- Dash, C.; Wang, G.; Muñoz-Castro, A.; Ponduru, T. T.; Zacharias, A. O.; Yousufuddin, M.; Dias, H. V. R., Organic Azide and Auxiliary-Ligand-Free Complexes of Coinage Metals Supported by N-Heterocyclic Carbenes. *Inorg. Chem.* 2020, 59, 2188-2199
- 49. Waterman, R.; Hillhouse, G. L., η^2 -Organoazide Complexes of Nickel and Their Conversion to Terminal Imido Complexes via Dinitrogen Extrusion. *J. Am. Chem. Soc.* **2008**, *130*, 12628-12629.
- 50. Harrold, N. D.; Hillhouse, G. L., Strongly bent nickel imides supported by a chelating bis(N-heterocyclic carbene) ligand. *Chem. Sci.* **2013**, *4*, 4011-4015.
- 51. Harrold, N. D.; Corcos, A. R.; Hillhouse, G. L., Synthesis, structures, and catalytic reactivity of bis(*N*-heterocyclic carbene) supported diphenyldiazomethane and 1-azidoadamantane complexes of nickel. *J. Organomet. Chem.* **2016**, *813*, 46-54.
- 52. Proulx, G.; Bergman, R. G., Synthesis and Structure of a Terminal Metal Azide Complex: An Isolated Intermediate in the Formation of Imidometal Complexes from Organic Azides. *J. Am. Chem. Soc.* **1995**, *117*, 6382-6383.
- 53. Proulx, G.; Bergman, R. G., Synthesis, Structures, and Kinetics and Mechanism of Decomposition of Terminal Metal Azide Complexes: Isolated Intermediates in the Formation of Imidometal Complexes from Organic Azides. *Organometallics* 1996, 15, 684-692.
- 54. Fickes, M. G.; Davis, W. M.; Cummins, C. C., Isolation and Structural Characterization of the Terminal Mesityl Azide Complex V(N₃Mes)(I)(NRAr_F)₂ and Its Conversion to a Vanadium(V) Imido Complex. *J. Am. Chem. Soc.* **1995**, *117*, 6384-6385.
- 55. Harman, W. H.; Lichterman, M. F.; Piro, N. A.; Chang, C. J., Well-Defined Vanadium Organoazide Complexes and Their Conversion to Terminal Vanadium Imides: Structural Snapshots and Evidence for a Nitrene Capture Mechanism. *Inorg. Chem.* 2012, 51, 10037-10042.
- 56. Obenhuber, A. H.; Gianetti, T. L.; Berrebi, X.; Bergman, R. G.; Arnold, J., Reaction of (Bisimido)niobium(V) Complexes with Organic Azides: [3+2] Cycloaddition and Reversible Cleavage of β -Diketiminato Ligands Involving Nitrene Transfer. *J. Am. Chem. Soc.* **2014**, *136*, 2994-2997.
- 57. Abu-Omar, M. M.; Shields, C. E.; Edwards, N. Y.; Eikey, R. A., On the Mechanism of the Reaction of Organic Azides with Transition Metals: Evidence for Triplet Nitrene Capture. *Angew. Chem., Int. Ed.* **2005**, *44*, 6203-6207.

- 58. Guillemot, G.; Solari, E.; Floriani, C.; Rizzoli, C., Nitrogen-to-Metal Multiple Bond Functionalities: The Reaction of Calix[4]arene–W(IV) with Azides and Diazoalkanes. *Organometallics* **2001**, *20*, 607-615.
- 59. Wu, H.; Hall, M. B., A New Mechanism for the Conversion of Transition Metal Azides to Imido Complexes. *J. Am. Chem. Soc.* **2008**, *130*, 16452-16453.
- 60. Travia, N. E.; Xu, Z.; Keith, J. M.; Ison, E. A.; Fanwick, P. E.; Hall, M. B.; Abu-Omar, M. M., Observation of Inductive Effects That Cause a Change in the Rate-Determining Step for the Conversion of Rhenium Azides to Imido Complexes. *Inorg. Chem.* 2011, 50, 10505-10514.
- 61. Ghosh, S.; Baik, M.-H., Mechanism of Redox-Active Ligand-Assisted Nitrene-Group Transfer in a Zr^{IV} Complex: Direct Ligand-to-Ligand Charge Transfer Preferred. *Chem. Eur. J.* **2015**, *21*, 1780-1789.
- 62. Hanna, T. A.; Baranger, A. M.; Bergman, R. G., Addition of Organic 1,3-Dipolar Compounds across a Heterobinuclear Bond between Early and Late Transition Metals: Mechanism of Nitrogen Loss from an Organoazido Complex To Form a Bridging Imido Complex. Angew. Chem., Int. Ed. Engl. 1996, 35, 653-655
- Curley, J. J.; Bergman, R. G.; Tilley, T. D., Preparation and physical properties of early-late heterobimetallic compounds featuring Ir–M bonds (M = Ti, Zr, Hf). *Dalton Trans.* 2012, 41, 192-200.
- 64. Reinholdt, A.; Pividori, D.; Laughlin, A. L.; DiMucci, I. M.; MacMillan, S. N.; Jafari, M. G.; Gau, M. R.; Carroll, P. J.; Krzystek, J.; Ozarowski, A.; Telser, J.; Lancaster, K. M.; Meyer, K.; Mindiola, D. J., A Mononuclear and High-Spin Tetrahedral Ti^{II} Complex. *Inorg. Chem.* **2020**, *59*, 17834–17850.
- Franceschi, F.; Solari, E.; Floriani, C.; Rosi, M.; Chiesi-Villa, A.; Rizzoli, C., Molecular Batteries Based on Carbon–Carbon Bond Formation and Cleavage in Titanium and Vanadium Schiff Base Complexes. *Chem. Eur. J.* 1999, 5, 708-721.
- 66. Mullins, S. M.; Duncan, A. P.; Bergman, R. G.; Arnold, J., Reactivity of a Titanium Dinitrogen Complex Supported by Guanidinate Ligands: Investigation of Solution Behavior and a Novel Rearrangement of Guanidinate Ligands. *Inorg. Chem.* 2001, 40, 6952-6963.
- 67. Hanna, T. E.; Keresztes, I.; Lobkovsky, E.; Bernskoetter, W. H.; Chirik, P. J., Synthesis of a Base-Free Titanium Imido and a Transient Alkylidene from a Titanocene Dinitrogen Complex. Studies on Ti=NR Hydrogenation, Nitrene Group Transfer, and Comparison of 1,2-Addition Rates. *Organometallics* 2004, 23, 3448-3458.
- 68. Cavaliere, V. N.; Crestani, M. G.; Pinter, B.; Pink, M.; Chen, C.-H.; Baik, M.-H.; Mindiola, D. J., Room Temperature Dehydrogenation of Ethane to Ethylene. *J. Am. Chem. Soc.* **2011**, *133*, 10700-10703.
- 69. Clark, K. M., Synthesis and Reactivity of Low-Coordinate Titanium Synthons Supported by a Reduced Redox-Active Ligand. *Inorg. Chem.* **2016**, *55*, 6443-6448.
- 70. Heins, S. P.; Wolczanski, P. T.; Cundari, T. R.; MacMillan, S. N., Redox non-innocence permits catalytic nitrene carbonylation by (dadi)Ti=NAd (Ad = adamantyl). *Chem. Sci.* **2017**, *8*, 3410-2418
- 71. Fischer, M.; Wolff, M. C.; del Horno, E.; Schmidtmann, M.; Beckhaus, R., Synthesis, Reactivity, and Insights into the Lewis Acidity of Mononuclear Titanocene Imido Complexes Bearing Sterically Demanding Terphenyl Moieties. *Organometallics* **2020**, *39*, 3232–3239.
- Aguilar-Calderón, J. R.; Murillo, J.; Gomez-Torres, A.; Saucedo, C.; Jordan, A.; Metta-Magaña, A. J.; Pink, M.; Fortier, S., Redox Character and Small Molecule Reactivity of a Masked Titanium(II) Synthon. *Organometallics* 2020, 39, 295-311.
- 73. Graham, T. W.; Kickham, J.; Courtenay, S.; Wei, P.; Stephan, D. W., Reduction of Titanium(IV)-Phosphinimide Complexes:

- Routes to Ti(III) Dimers, Ti(IV)-Metallacycles, and Ti(II) Species. *Organometallics* **2004**, *23*, 3309-3318.
- 74. Boynton, J. N.; Guo, J.-D.; Grandjean, F.; Fettinger, J. C.; Nagase, S.; Long, G. J.; Power, P. P., Synthesis and Characterization of the Titanium Bisamide Ti{N(H)Ar^{iPr6}}₂ (Ar^{iPr6} = C₆H₃-2,6-(C₆H₂-2,4,6-ⁱPr₃)₂ and Its TiCl{N(H)Ar^{iPr6}}₂ Precursor: Ti(II) → Ti(IV) Cyclization. *Inorg. Chem.* **2013**, *52*, 14216-14223.
- Aguilar-Calderón, J. R.; Metta-Magaña, A. J.; Noll, B.; Fortier, S., C(sp³)-H Oxidative Addition and Transfer Hydrogenation Chemistry of a Titanium(II) Synthon: Mimicry of Late-Metal Type Reactivity. *Angew. Chem., Int. Ed.* 2016, 55, 14101-14105.
- 76. Gómez-Torres, A.; Aguilar-Calderón, J. R.; Saucedo, C.; Jordan, A.; Metta-Magaña, A.; Pinter, B.; Fortier, S., Reversible oxidative-addition and reductive-elimination of thiophene from a titanium complex and its thermally-induced hydrodesulphurization chemistry. *Chem. Commun.* 2020, 56, 1545-1548.
- 77. Walsh, P. J.; Hollander, F. J.; Bergman, R. G., Monomeric and dimeric zirconocene imido compounds: synthesis, structure, and reactivity. *Organometallics* **1993**, *12*, 3705-3723.
- Cowley, R. E.; Golder, M. R.; Eckert, N. A.; Al-Afyouni, M. H.; Holland, P. L., Mechanism of Catalytic Nitrene Transfer Using Iron(I)–Isocyanide Complexes. *Organometallics* 2013, 32, 5289-5298.
- 79. Yousif, M.; Tjapkes, D. J.; Lord, R. L.; Groysman, S., Catalytic Formation of Asymmetric Carbodiimides at Mononuclear Chromium(II/IV) Bis(alkoxide) Complexes. *Organometallics* **2015**, *34*, 5119-5128.
- 80. Beaumier, E. P.; McGreal, M. E.; Pancoast, A. R.; Wilson, R. H.; Moore, J. T.; Graziano, B. J.; Goodpaster, J. D.; Tonks, I. A., Carbodiimide Synthesis via Ti-Catalyzed Nitrene Transfer from Diazenes to Isocyanides. *ACS Catal.* **2019**, *9*, 11753-11762.
- 81. Reinholdt, A.; Jafari, M. G.; Sandoval-Pauker, C.; Ballestero-Martínez, E.; Gau, M. R.; Driess, M.; Pinter, B.; Mindiola, D. J., Phosphorus and Arsenic Atom Transfer to Isocyanides to Form π-Backbonding Cyanophosphide and Cyanoarsenide Titanium Complexes. *Angew. Chem., Int. Ed.* **2021**, *60*, 17595-17600.
- 82. Addison, A. W.; Rao, T. N.; Reedijk, J.; van Rijn, J.; Verschoor, G. C., Synthesis, Structure, and Spectroscopic Properties of Copper(II) Compounds Containing Nitrogen–Sulphur Donor Ligands; The Crystal and Molecular Structure of Aqua[1,7-bis(*N*-methylbenzimidazol-2'-yl)-2,6-dithiaheptane]copper(II) Perchlorate. *J. Chem. Soc., Dalton Trans.* 1984, 1349-1356.
- 83. Pyykkö, P.; Atsumi, M., Molecular Single-Bond Covalent Radii for Elements 1–118. *Chem. Eur. J.* **2009**, *15*, 186-197.
- 84. Pyykkö, P.; Atsumi, M., Molecular Double-Bond Covalent Radii for Elements Li–E112. *Chem. Eur. J.* **2009**, *15*, 12770-12779.
- 85. Parr, R.G.; Yang, W. Density Functional Theory of Atoms and Molecules. Oxford University Press: New York, **1989**.
- 86. Perdew, J. P.; Burke, K.; Ernzerhof, M. Generalized gradient approximation made simple *Phys. Rev. Lett.* **1996**, *77*, 3865-3868
- 87. Grimme, S.; Antony, J.; Ehrlich, S.; Krieg, S. A consistent and accurate ab initio parametrization of density functional dispersion correction (DFT-D) for the 94 elements H-Pu. *J. Chem. Phys.* **2010**, *132*, 154104.
- 88. Hay, P. J.; Wadt, W. R. Ab Initio Effective Core Potentials for Molecular Calculations. Potentials for the Transition Metal Atoms Sc to Hg. *J. Chem. Phys.* **1985**, *82*, 270-283.
- 89. Wadt, W. R.; Hay, P. J. Ab Initio Effective Core Potentials for Molecular Calculations. Potentials for Main Group Elements Na to Bi. *J. Chem. Phys.* **1985**, *82*, 284-298.
- Hay, P. J.; Wadt, W. R. Ab Initio Effective Core Potentials for Molecular Calculations. Potentials for K to Au Including the Outermost Core Orbitals. J. Chem. Phys. 1985, 82, 299-310.
- 91. Slater, J. C. The Self-Consistent Field for Molecules and Solids: Quantum Theory of Molecules and Solids; McGraw-Hill Book Company, **1974**.

- 92. Ison, E. A.; Cessarich, J. E.; Travia, N. E.; Fanwick, P. E.; Abu-Omar, M. M., Synthesis of Cationic Rhenium(VII) Oxo Imido Complexes and Their Tunability Towards Oxygen Atom Transfer. *J. Am. Chem. Soc.* **2007**, *129*, 1167-1178.
- 93. Dunkin, I. R.; Shields, C. J.; Quast, H.; Seiferling, B., The photolysis of 1-azido-4-methylbicyclo[2.2.2]octane and 1-azidoadamantane in low-temperature matrices. *Tetrahedron Lett.* **1983**, *24*, 3887-3890.
- 94. Radziszewski, J. G.; Downing, J. W.; Jawdosiuk, M.; Kovacic, P.; Michl, J., 4-Azahomoadamant-3-ene: spectroscopic characterization and photoresolution of a highly reactive strained bridgehead imine. *J. Am. Chem. Soc.* **1985**, *107*, 594-603
- 95. Wayne, G. S.; Snyder, G. J.; Rogers, D. W., Measurement of the strain energy of a transient bridgehead imine, 4-azahomoadamant-3-ene, by photoacoustic calorimetry. *J. Am. Chem. Soc.* **1993**, *115*, 9860-9861.

TOC Graphic

